Statistical Analysis on Wall Shear Stress of Turbulent Boundary Layer in a Channel Flow using Micro Shear Stress Imager

Norimasa Miyagi, Motoaki Kimura, Hideo Shoji, Atsusi Saima
Department of Mechanical Engineering, College of Science and Technology, Nihon University
1-8 Kanda Surugadai, Ciyoda-ku, Tokyo 101-8308, Japan

Chih-Ming Ho, Steve Tung
Mechanical and Aerospace Engineering Department, University of California, Los Angeles
Los Angeles, California 90095, USA

Yu-Chong Tai
Division of Engineering and Applied Science, California Institute of Technology
Pasadena, California 91125, USA

ABSTRACT

Measurements of wall shear stress of a turbulent boundary layers in the channel flow were carried out using MEMS-based micro shear stress imaging chip. The study was carried out in a turbulent channel flow facility. One array of 25 micro shear sensors in the chip that covers a length of 7.5 mm is used measure the instantaneous span-wise distribution of the surface shear stress. The characteristics of high shear-stress area (streaks) were described with statistics. Based on the measurement, the physical quantities associated with the high shear-stress streaks, such as their length, width with the high shear stress level, were obtained.

To further explore the relationship between the shear stress slope and the peak shear stress, the probability density function (PDF) of the ratio of peak shear stress to shear stress slope at different Reynolds number *Re* are examined. As for the distribution of PDF, it was found out that the distribution concentrated toward a certain value in each Re. This result is extremely important because it points to the possibility of predicting the peak shear stress level based on the share stress distribution at the leading edge of the streaks.

By multiplying the ratio of peak to slope of shear stress at the peak value of the PDF by the measured front-end slope of individual streaks, we can "predict" the peak value of the shear stress in real-time due to the correlation between the two values. We then can determine the necessary input driving level to the actuator for reducing the shear stress. This result will be implemented into the algorithm for the integrated turbulent boundary layer control system.

INTRODUCTION

The presence of near-wall streak structure in turbulent boundary layer has observed for many years in flow visualization and experimental investigation (Cantwell 1891, Kline et al. 1967, Kim, H. T et al. 1971, Falco 1980, Head et al. 1981, Smith et al. 1983). At high Reynolds number, Re, these streaks are typically very small in size and cannot be properly resolved by traditional measuring techniques. Numerical simulation indicate that the streaks are associated with stream wise vortices in the viscous sub-layer. The rotational motion of these vortices imposes high fluctuating surface shear stress on the wall (Kim, J. et al. 1987). There have been many measurement techniques for measuring shear stress. The hot-film technique and its variants have been widely used for the detailed investigation of fluctuating wall shear stress (Alfreadsson et al. 1988, Bruun 1995). The direction sensitive laser Doppler anemometer is a candidate, which enables to evaluate both magnitude and direction of the wall shear stress. An optical method proposed by Nquwi and Reynolds (1991) is supposed to be capable of measuring the wall shear stress with high spatial resolution. No matter the instrument, the requirements of fine spatial resolution, fast frequency response, high sensitivity and convenience need to be satisfied for turbulent boundary layer research.

Recently, the availability of a new manufacturing process, micro-electro-mechanical-system (MEMS) technology, has offered the possibility of sensing and controlling the small near-wall streaks (Ho et al. 1997). A multidisciplinary research collaboration between UCLA and Caltech has undergone to design and fabricate a large-scale distribution control system with integrated micromachined transducer and microelectronic circuits for surface shear stress control in turbulent boundary layers (Tung et al. 1995, Ho et al. 1996). The principal aim is to develop a real-time micro system that consists of large number of shear stress sensors and actuators integrated with the neural network control circuit. In this paper, our effort is directed to qualifying the characteristics of near-wall streaks and providing control guideline for the control system. First, this paper presents the micro shear stress sensor and measurement. Secondly, the

performance of a micro shear stress sensor is compared with the existing experimental data. Thirdly, the characteristics and the several statistical results of shear stress streaks are presented, and the information of shear stress streaks is taken up for predicting the shear stress peak level with concrete numerical value.

FACILITY AND MICRO SHARE STRESS IMAGING CHIP

Experimental Setup

The study was carried out in a turbulent channel flow facility. The channel constructed of 13[mm] Plexiglas, is 610[mm] x 25.4[mm] in cross-section and 4880[mm] long. An axial blower controlled by a DC power supply generates the air flow in the channel. Previous hot-wire measurement indicates that the channel flow, at a centerline velocity of 10[m/s], consists of a laminar entrance flow and a fully developed turbulent flow in the downstream half of the channel.

Micro Shear Stress Imaging Chip

A micro shear-stress imaging chip, which is composed of multiple micro shear stress sensor (Jiang et al. 1996), is exhibited in Fig.1. Five rows of the micro sensor were installed on the imaging chip, three of which contain 25 sensors each. Within each array, the distance between sensors is 300[μm]. The sensors are thermal types. Figure 2 shows top and cross-sectional views of a micro shear stress sensor. Each micro sensor consists of a 150[μm] long, 3[μm] wide, and 0.45[μm] thick polysilicon resistor wire and a 2[μm] deep vacuum cavity underneath. The purpose of the cavity is to reduce heat transfer from the resister wire to the substrate and increase the sensitivity of the sensor (Huang et al. 1996). The sensors are connected to external constant temperature mode circuit. Output signals from the anemometer circuits are digitized by a 64-channel Keithly Metrabyte ADC board in a Pentium 120 similar to a hot wire anemometer, through gold bonding wires and driven at an overheat ratio of 1.1 based PC. At a gain of 10, the sensitivity of the shear stress sensor is about 1[V/Pa] with a frequency response of 25[kHz]. The first array of 1-25 micro shear stress sensor that covers a distance of 7.5[mm] is used to measure the instantaneous spanwise distribution of the turbulent boundary surface shear stress. The experiment was carried out at Re ($=du_\infty/\nu$, where d is the half width of the channel, u_∞ is the centerline velocity) ranging from 8,758 to17,517.

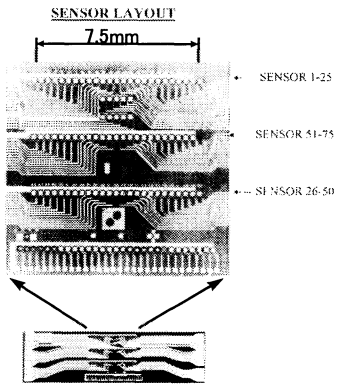

Fig.1 A micro shear-stress image chip

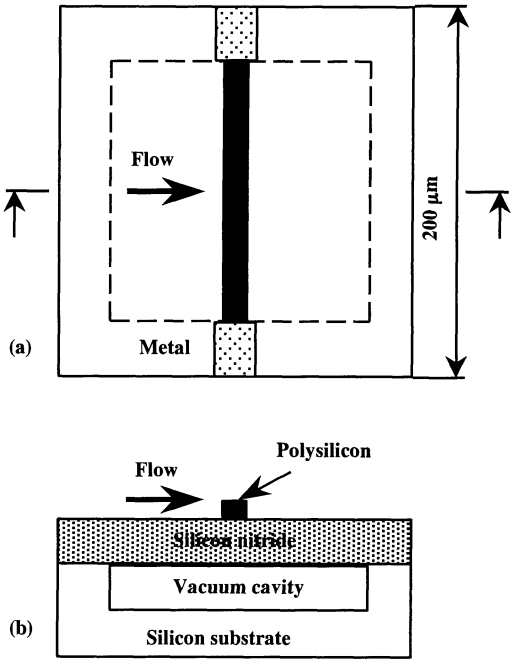

Fig.2 Schematic top:(a) and cross-section:(b) views of the micro shear stress sensor

Shear Stress Sensor Calibration and Temperature Compensation

The heating power of a shear stress sensor operating in steady state can be correlated with wall shear stress τ as follows (Bruun, 1995):

$$i^2R^2 = (T_f - T)(A + B\tau^{1/3}) \qquad (1)$$

Where T_f and T are the temperature of the sensor and the measured fluid, respectively, R is the resistance of the sensor, constants. The time-average signals from the sensors are calibrated against the time-average surface shear stress derived from the local pressure gradient. Temperature compensation was achieved first by collecting both ambient temperature and shear stress data, then, correcting accordingly with software after experiment.

RESULTS AND DISCCUSION

Shear-Stress Distribution

Fig.3 shows the contours of 2-D shear stress distribution measured by the 25 sensors covering an area 7.5[mm] in wide, 20[ms] in time for three time different *Re* numbers. Areas of high share stress are marked by light-gray in the plots while dark-gray represents low shear stress. Note that the transverse scale of the longitudinal high share-stress streaks varies with *Re* number increases. They also appear to have shorter the time length.

PDF of Wall Shear Stress

Based on the fluctuating share stress data measured during 2.5[sec] sampling time at 10[kHz] acquisition rate, the probability density functions (PDF) are calculated and shown in Fig.4. As the *Re* increases, the peak value of the PDF distribution shift towards the higher shear stress side, indicating an increase in the time-average shear stress level. The minimum shear stress level also changes with the *Re*. The PDF's are normalized and compared to those LGM (Laser Gradient Meter) by Obi et al.(1995) at *Re*=3300 (Fig.5). The non-dimensionalized shear stress τ^* is defined as:

$$\tau^* = (\tau - \tau_m)/\tau' \qquad (2)$$

Where τ_m is the time-average shear stress and τ' is the *rms* of share stress. The PDF's are normalized so that the integrated volume is unity. All the PDF's overlap one distribution and distribution agrees very well with the LGM's data. The performance of the micro shear stress sensor is examined by comparing the turbulent statistics measured by the micro sensor with that by previous experiments and computations. The root mean square, skewness factor and flatness factor of surface shear stress are 0.4, 1.09, and 4.6, respectively. The turbulence statistics measured by the micro sensor are in good agreement with previous experimental and numerical results (Obi, 1995).

High Share Stress Streaks

To investigate the characteristics of the high shear-stress streaks, a threshold of signal level is needed in order to separate the streaks from background fluctuations. This criterion should be able to 'mark' the high shear-stress area so that the streaks can be isolated. As τ^* is based on the ratio of the instantaneous 2-D shear-stress to the time-average level, τ^* is chosen to be the criterion. The best threshold level is decided by the two factors. One is the separation between high shear streaks to pick up from the shear stress sensor contour. Fig.6 shows the change streak areas that are identified according to different value of τ^*. Areas of high shear stress are marked by light gray plots while dark gray represents low shear stress. The area of high shear stress streaks decreases as τ^* number increases. The order is the signal level to distinguish between high shear stress streaks and the background fluctuation.

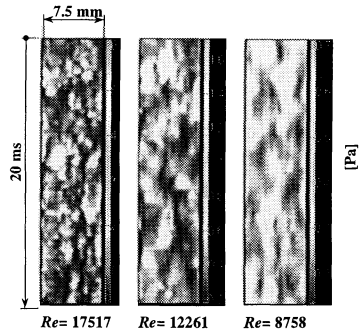

Fig.3 Instantaneous surface shear-stress measured by the imaging chip.

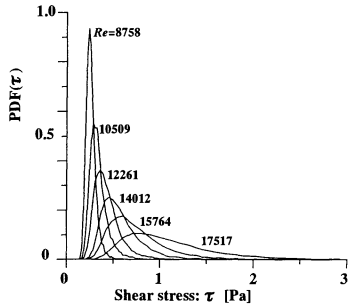

Fig.4 PDF of shear stress at different Reynolds number

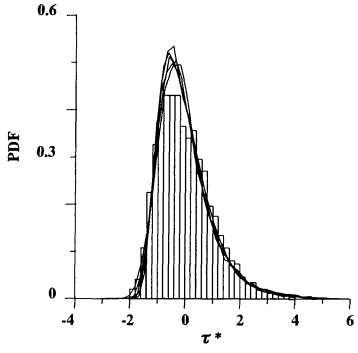

Fig.5 Normalized PDF; the bar chart is by Obi et al. (1995) and the solid lines are measured by the micro shear stress sensor

The low value of τ^* is better to predict high shear-stress peak in the early stage of high shear-stress streaks. Fig.7 shows the normalized time trace of the shear-stress streaks for different *Re*. The traces are the ensemble averages of the 'Center' trace of a shear-stress streaks. The sensor that detect the peak shear stress of a streak measures the 'Center' trace.

The figure shows that the normalized peak levels of shear-stress streaks are almost same in spite of the different *Re*, it is determined that a τ^* value of 0.3 is the best threshold level in identifying the structures because of the shear-stress streaks separation.

Definition of Peak, Length and Slope of Streaks

One of the aims of studying the 2-D shear stress distribution is to develop an identification criterion that can be used by control logic circuit to detect the passage of the high shear-stress streaks. To develop such a criterion, the characteristics of the streaks, length, peak shear-stress levels and shear-stress slopes are examined.

Peak, length and slope of high shear stress streaks are illustrated in Fig.8. The peak is defined as the maximum shear stress in the streak. The length defined as the streak length in time of limit above $\tau^* = 0.3$. The threshold $\tau^* = 0.3$ is decided by the area separation of high shear stress streaks to pick up high shear stress streaks, and the background fluctuation level of shear stress as mentioned in section High Shear Stress Streaks. The slope is defined as the front-end (30% of the streaks length in time) shear stress gradient of the streak. It is to be desired that the time is as short as possible to predict the peak in early stage. A streak has spread out in two dimension, so that it has several slopes in front-end. In this way, the slope is maximum- slope in a streak.

Statistical Characteristics of Streaks

Figures 9 to 11 show the PDFs of several shear stress streaks characteristics at different *Re*. Fig.9 show s the PDF of the shear-stress peak at different *Re* number. As the *Re* increases, the peak average increases from 0.4 to 2.5[Pa], and the distribution becomes wider. Fig.10 shows the PDF of the streak time length at different *Re* As the *Re* increases, the average streak time length decreases from 2.5 to 1.5[ms], and its distribution becomes narrower. Figure 11 shows the PDF of the shear stress slope. For *Re*=8758, the slope distribution is concentrated in a small area. As the *Re* increases, the average shear-stress slope increases from 2.0 to 7.0[Pa/ms], and the distribution becomes winder.

Prediction of Peak Shear-Stress

To explore the relationship between the shear stress slope and the peak shear stress, the PDF of the ratio of peak shear stress to shear stress slope at different *Re* are examined. As shown in Fig.12, the PDF distributions for all *Re* cases have a peak in a narrow range, indicating the existence of a preferred ratio. The peak value of the PDF decreases with increasing *Re* number. The highest probability ratio *Rp* in each *Re* numbers are 0.5[Pa/Pa/ms] (*Re*=17517), 0.5[Pa/Pa/ms] (*Re*=12261), 1.0[Pa/Pa/ms] (*Re*=8758) respectively. The ratio interval *Rp*±0.4[Pa/Pa/ms] covers probability of the ratio distribution greater than 60%.

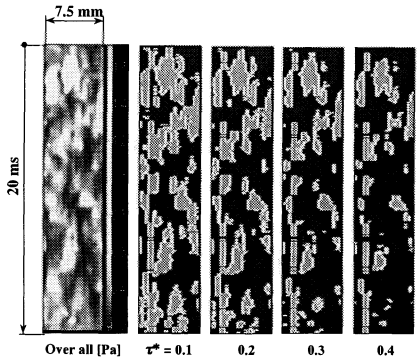

Fig.6 Change of high shear stress area on τ^* number

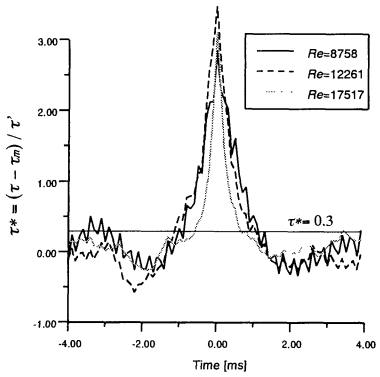

Fig.7 Ensemble averaged time trace of high shear stress streak and threshold.

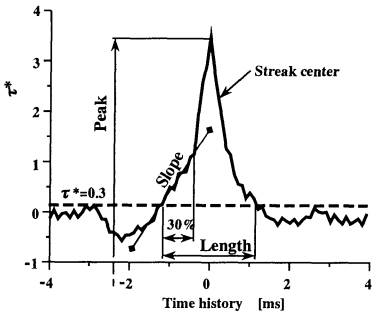

Fig.8 Peak, Length and Slope of streaks

By multiplying this ratio (peak to slope of shear stress at the peak value of the PDF) by the measured front-end slope of individual streaks, we can "predict" the peak value of the shear stress in real-time due to the correlation between the two values. This result is extremely important because it points to the possibility of predicting the peak shear-stresslevel based on the shear-stress distribution at the leading edge of the streaks.

CONCLUSION

A micromachined surface shear-stress imaging chip was used to measure the instantaneous shear-stress distribution on the wall in a turbulent boundary layer. The statistics associated with near-wall high shear stress streaks were studied. To investigate the characteristic of the high shear-stress streaks, we first determined a threshold to separate the streak from the background fluctuation. Several characteristics of the shear stress streaks, such as the length, the width the front-end slope, and the shear stress peak are obtained at different *Re*.

In particular, reasonable correlation between the peek shear stress and its front-end slope of a streaks is established. It was further shown that the ratio of the peak shear stress to the front-end slope of shear stress streaks has sharp peak in its probability density distribution. The peak value of the PDF decrease with increasing *Re* number. These two findings are extremely important. By multiplying this ratio (Peak to Slope of shear stress at the peak value of the PDF) by the measured front-end slope of individual streaks, we can "predict" the peak value of the shear stress in real-time due to the correlation between the two values. We then can determine the necessary input driving level to the actuator for reducing the shear stress. This result will be implemented into the algorithm for the integrated turbulent boundary layer control system.

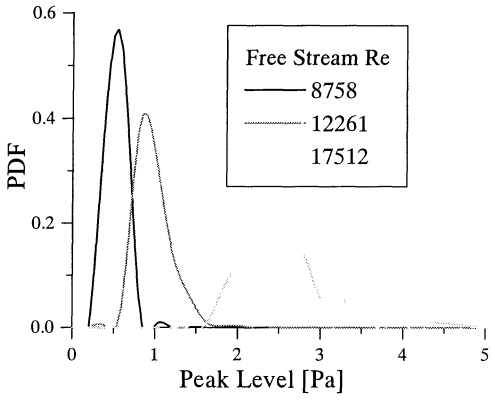

Fig 9 PDF of peak of the high shear stress streak at the different Re's

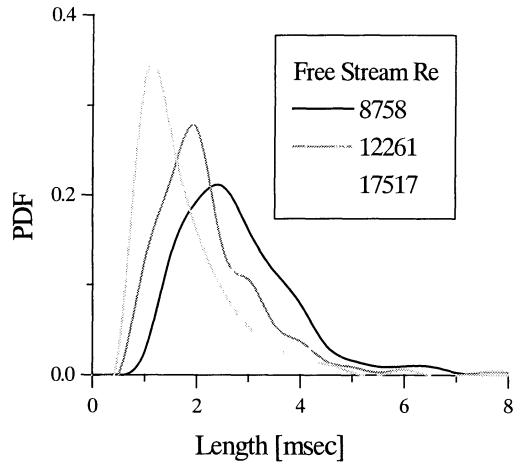

Fig 10 PDF of length in time of the high shear stress streak at the different Re.

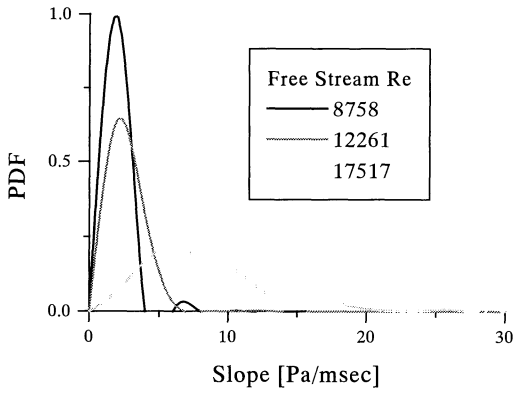

Fig 11 PDF of slope of the shear stress streak at the different Re's.

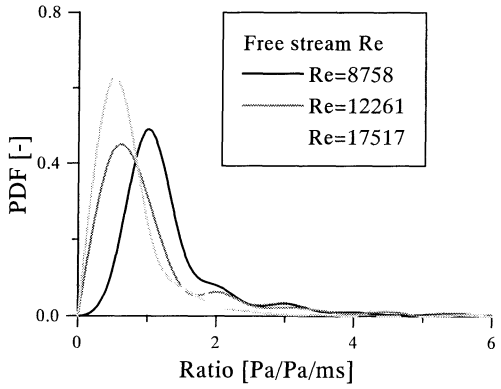

Fig 12 The Ratio of peak shear-stress to shear-stress gradient at different Re's

ACKNOWLEDGMENTS

This work is supported by an URI project from US Air Force Office of Scientific Research. The exchange visitor program UCLA, USA and Nihon University, Japan support M. Kimura. We also appreciate the help from Mr. J. Lew. of UCLA, USA and Mr. J. Hoffelner of University of Linz, Austria.

REFERENCE

Alfreadsson, P.H., Johnansson, A.V., Haritonidis, J.H. and Eckelmann, H., 1988, "The Fluctuating Wall-Shear Stress and the Velocity field in the Viscous Sublayer," Phys. Fluids 31 (5), pp. 1026-1033.

Bruun, H. H., 1995, "Hot-Wire Anemometry," Oxford University Press, pp.272-286.

Cantwell, B.J., 1981, "Organized Motion in Turbulent Flow," Ann. Rev. FluideMech., Vol.13, pp.457-515.

Falco, R., 1980, "The Production of Turbulence Near a Wall," AIAA Paper, 80-1356.

Head, M. R. and Bandyopadhyay, P., 1981 "New Aspects of Turbulent Boundary-Layers Structure," J. Fluid Mech. Vol.107, pp.297-338.

Ho, C. M., Tung, S. and Tai, Y. C., 1996, "Intarctive Control of Wall Structure by MEMS-Based Transducers," Advance In Turbulence, *Proceedings of the Sixth European Turbulence Conference*,pp.413, Lausanne, Switzerland, July

Ho, C.M., Tung, S. and tai, Y. C., Jiang, F. and Tsao, T, 1997, "MEMS- A Technology for advancements in Aerospace Engineering," AIAA Paper 97-0545.

Huage, J. B., Tung, S., Ho, C. H., Liu, C., and Tai, Y.C., 1996, "Improved Micro Thermal Shear-Stress Sensor," IEEE transactions on Instrumentation and Measurements, Vol.45, No.2, pp.570

Jiang, F., Tai, Y. C., Gupta, B., Goodman, R., Tung, S., Huang, J. B. and Ho, C. M., 1996, "A Surface-Micromachined Shear Stress Imager," *proceedings of the 9th International IEEE Workshop on MEMS,* p.110, San Diego.

Kim, H.T., Kline, S J., Reynolds, W.C., 1971, "The Production of Turbulence Near a Smooth Wall in a Turbulent Boundary Layer," J. Fluide Mech. Vol.50, Part1, pp.133-160.

Kim, J., Moin, P. and Moser, R., 1987, "Turbulant statistics in Fully developed Channel Flow at Low Reynolds Number," J.Fluide Mech. Vol.50, Part1, pp.133-160.

Kline, S J., Reynolds, W.C., Schraub, F. A. and Runstadler, P.W., 1967, "The Structure of Turbulent Boundary layers." J. Fluid Mech., Vol.30, Part 4, pp.741-773.

Naqwi, A.A. and Reynolds, W.C., 1991, "Measurement of Turbulent Wall Velocity Gradient using Cylindrical Waves of Laser Light," Experiments in Fluids, Vol.10, pp.257-266.

Obi, S., Inoue, K., Furukawa, T, and Masuda, S, 1995,"Experimental Study on the Statistics of Wall Shear Stress in Turbulent Channel Flows," *Proceedings of 10th Symposium on Turbulent Shear Flows,* Vol.1, p.5-19-5-24

Smith, C. R. and Metzler, S. P., 1983, "The Characteristics of low-Speed streaks in the Near-Wall region of a Turbulent Boundary Layer," J. Fluid Mech. Vol.129, pp.27-54.

Tung, S., Hong, H., Huang, j.b., Ho, C. M., Liu, C. and Tai, Y. C., 1995, "Control of a Streamwise Vortex by a Mechanical Actuator," *Proceedings of 10th Symposium on Turbulent Shear Flows,* Vol.1, pp.1-19, Pennsylvania, USA, August.